



Research article

Novel diagnostic indicators for acute angle closure secondary to lens subluxation based on anterior segment and lens parameters

Yizhen Tang^{a,b,1}, Yan Gao^{a,b,1}, Xiaowei Yu^{a,b}, Hongyu Zhong^{a,b}, Guanchen Gong^c, Feng Mei^{a,b}, Zhigang Fan^{a,b,**}, Yan Shi^{a,b,*}

^a Department of Ophthalmology, Beijing Tongren Hospital, Capital Medical University, Beijing Ophthalmology & Visual Sciences Key Laboratory, Beijing, 100730, China

^b Institute of Ophthalmology, Beijing Ophthalmology & Visual Sciences Key Laboratory, Capital Medical University, Beijing, 100730, China

^c Department of Ophthalmology, Zhangjiajie People's Hospital, Zhangjiajie, China

ARTICLE INFO

Keywords:

Acute angle closure
Lens subluxation
Diagnostic indicator
Anterior segment
Crystalline lens

ABSTRACT

Purpose: To explore stable and sensitive indicators for clinical diagnosis of acute angle closure (AAC) secondary to lens subluxation (LS) through quantitative analysis of CASIA 2 imaging.

Design: A prospective cross-sectional study.

Methods: Setting: Clinical practice.

Participants: 23 patients with unilateral acute angle closure secondary to lens subluxation and 23 cataract patients without lens subluxation were recruited. Lens subluxation was confirmed by ultrasound biomicroscope diagnosis. The contralateral eyes without LS served as fellow control group. The cataract eyes without LS were enrolled in blank control group.

Intervention: Participants underwent ophthalmologic examinations including slit-lamp biomicroscope, best corrected visual acuity, intraocular pressure, central corneal thickness measurement, axial length, gonioscopy, ultrasound biomicroscope and 360-degree anterior chamber and crystalline lens scan protocols of CASIA 2 system.

Main outcome measures: Automated circumferential anterior segment and lens morphological parameters under anterior segment optical coherence tomography were analyzed via three-dimensional analysis.

Results: Significant differences were found in the front and back radius of the lens, the front and back radius of steep curvature of the lens, lens thickness, lens decentration, lens diameter, iris-trabecular contact (ITC) index, ITC area, anterior chamber depth (ACD), lens vault (LV), and iris volume between LS and controls. Among these parameters, LV, the anterior radius of steep curvature of the lens and ACD demonstrated the highest prediction power (AUC = 0.87, 0.89, and 0.86, respectively). The prediction power of tilt/axis was much higher in the Gaussian Naive Bayes model (AUCs = 0.90) than in the logistic model (AUCs = 0.74). Combination of LV_mean, LV_std, tilt and tilt axis in Gaussian Naive Bayes model presented as most stable and excellent diagnostic markers for AAC secondary to LS (AUCs = 0.98).

* Corresponding author. Beijing Tongren Eye Center Research Ward, Beijing Tongren Hospital, Beijing Institute of Ophthalmology, Beijing Ophthalmology & Visual Sciences Key Laboratory, Capital Medical University, Beijing, 100730, China.

** Corresponding author. Beijing Tongren Eye Center Research Ward, Beijing Tongren Hospital, Beijing Institute of Ophthalmology, Beijing Ophthalmology & Visual Sciences Key Laboratory, Capital Medical University, Beijing, 100730, China.

E-mail addresses: fanzhigang@mail.ccmu.edu.cn (Z. Fan), yansmile4433@163.com (Y. Shi).

¹ The authors contribute equally.

<https://doi.org/10.1016/j.heliyon.2024.e25164>

Received 23 July 2023; Received in revised form 11 January 2024; Accepted 22 January 2024

Available online 26 January 2024

2405-8440/© 2024 The Authors. Published by Elsevier Ltd. This is an open access article under the CC BY-NC-ND license (<http://creativecommons.org/licenses/by-nc-nd/4.0/>).

Conclusions: The combination of markers including lens tilt and lens vault in the mathematic model facilitate clinical work as it not only provides novel diagnostic indications and possible prompt treatment for AAC secondary to lens subluxations, but also enhances our understanding of the pathogenic role of zonulopathy in angle closure glaucoma.

1. Introduction

Lens subluxation (LS) is an ocular disease in which the position of the lens shifts from its normal place due to abnormal development, rupture or relaxation of the suspensory ligaments. It could result from various factors such as trauma, genetic disorders, and age-related changes [1]. The dislocation of the crystalline lens affects visual function, leading to distorted or blurred vision, impairment of cornea endothelial cells and even elevated intraocular pressure [2–6]. Lens subluxation is a common disorder but sometimes difficult to diagnose accurately. Only 29.2 % of abnormal zonular ligaments could be diagnosed before combined glaucoma and cataract surgery [7]. If left untreated, lens subluxation can progress to a complete dislocation, where the lens move entirely out of its normal position, leading to acute angle closure (AAC) or even retinal injury. It's reported that approximately 18 % acute primary angle closure (APAC) [5] or primary angle closure glaucoma (PACG) [8] had spontaneous lens dislocation. About 6 % acute angle-closure glaucoma (ACG) secondary to lens subluxation were reported misdiagnosed as acute primary angle-closure glaucoma [8,9]. Moreover, lens subluxation also increases the risks and complications of cataract surgery including posterior capsule rupture, vitreous prolapse of nucleus and prolonged operation time. Therefore, accurate evaluation and early detection of lens subluxation are crucial for effective treatment and prevention of further complications.

Accurate imaging diagnosis of lens subluxation has always been a clinical concern. The current detection method was to visualize the position of the lens and to identify the distance between ciliary body and crystalline lens in four quadrants via ultrasound biomicroscope (UBM) [5,6,10]. However, since the anatomic location of zonules and the attachment position of the lens and ciliary process often varies. There exists a learning curve and often rely on the experiences of the technicians [11], which brings challenges to UBM diagnosis. As the development of new generation of swept-source anterior segment optical coherence tomography (ASOCT), CASIA2 system emerged as an advanced imaging device to capture high-resolution images with deeper and wider scanning of the anterior segment and crystalline lens, allowing for quantitative details of the lens position [12–16] including lens tilt, decentration, front and back curvature radius of lens and 360-degree angle parameters. What's more, no direct contact with the eye is needed, which decreases the risk of pre-operation infection and presents as an optimal detection method for lens subluxation. However, the application of CASIA2 ASOCT in the diagnosis of lens subluxation has not been widely investigated so far.

Consequently, a prospective study was conducted with LS patients confirmed by UBM. The LS patients enrolled in the study were acute angle closure patients secondary to LS. We aimed to analyze the anterior segment and lens morphological parameters between controls and lens subluxation patients using the CASIA2 system, and to explore novel indicators for the detection and diagnosis of acute angle closure secondary to lens subluxation in this study.

2. Methods

2.1. Study participates

This was a prospective observational study. Participants were recruited between December 2021 to December 2022 from Beijing Tongren Eye Center of Capital Medical University. The present study was approved by the Ethics Committee of Clinical Research in Beijing Tongren Hospital (TRECKY2020-056) of Capital Medical University and adhered to the Declaration of Helsinki. The informed consent was obtained from patients prior to conducting the research. Patients underwent ophthalmologic examinations including slit-lamp biomicroscope, best corrected visual acuity (BCVA), intraocular pressure (IOP) measurement, central corneal thickness (CCT) measurement, axial length (AL), gonioscopy, UBM and ASOCT. Demographic information such as age, gender was also documented.

The criteria for the patients enrolled in the present study were as following: 1) Patients with unilateral LS eye were enrolled. The LS eye was enrolled in LS group. All the eyes in LS group had an acute attack of angle closure secondary to LS with or without prolonged IOP elevation. The criteria for diagnosing LS are as following: asymmetrical distance between ciliary body and crystalline lens in different quadrants together with shallow central and peripheral anterior chamber depth, tilting of lens, asymmetrical anterior chamber depth in the same eye, and/or asymmetrical iris configuration [6] (Fig. S1). All the LS eyes were confirmed with UBM diagnosis by experienced technicians in the present study. 2) The criteria of the fellow control group are as below: The contralateral eye of the LS-eye without any symptoms of LS under UBM were enrolled in the fellow control group. The fellow eyes have no history of IOP elevation. 3) The cataract eyes without LS were enrolled in blank control group. 4) All the eyes haven't been treated with any ocular surgeries before examination including laser treatment. 6) All the patients with secondary or additional systematic diseases are excluded.

2.2. Anterior segment optical coherence tomography and crystalline lens parameters

The scan protocols of anterior chamber and crystalline lens in CASIA2 system were conducted as previously reported [16]. The scan had a length of 16 mm and a depth of 13 mm. Images were obtained over the duration of 5 s when the patient was focusing on an

internal target. A total of 16 ASOCT images from 360-degree angles were analyzed via three-dimensional analysis. Any image affected by motion or lid artifacts was excluded from the analysis. Automated circumferential angle parameters were collected. To align with the four quadrants (nasal, superior, temporal and inferior) of the right eyes, a counterclockwise rotation was applied from 0° to 360° (as shown in Fig. 3). The left eyes were mirror-transformed to match the right eyes.

The anterior chamber and crystallines lens parameters (anterior chamber depth (ACD), anterior chamber width (ACW), iris-trabecular contact (ITC) index, ITC area, the radius of the front curvature of lens (R[Front]), the radius of the back curvature of lens (R[Back]), the radius of the steep curvature of the lens(Rs), the radius of the flat curvature of the lens (Rf), lens decentration, and lens tilt) were assessed and analyzed. These parameters are defined as reported in previous literatures [17–20]. The schematic diagram was shown in Fig. S1. Additionally, the lens vault (the vertical distance from the anterior lens to the horizontal line between two scleral spurs, LV), lens diameter (diameter of equator part of the lens) and lens thickness (LT along vertex normal) were also measured and further processed by inbuilt semi-automated software. The determination of scleral spurs were conducted by two independent ophthalmologists.

Table 1
The characteristics of the included eyes.

	LS	Fellow(F)	Blank(B)	p_value*	p_value (LS vs F)	AUC (LS vs F)	AUC (LS vs F + B)
Basic information							
Gender (F%)	47.8		60.1	0.239			
Age (yr)	60.17 ± 8.57		66.52 ± 9.1	0.027		0.5	0.537
BCVA (logMAR)	0.39 ± 0.26	0.8 (0.6, 0.9)	0.48 ± 0.27	<0.001	0.001	0.83	0.639
IOP (mmHg)	21.01 ± 11.07	15.35 (13.6, 17.15)	14.9 (12.0, 16.0)	0.082	0.015	0.638	0.639
C/D	0.52 ± 0.23	0.43 ± 0.19	0.47 (0.3, 0.8)	0.888	0.033	0.584	0.36
Anterior segment							
ITC Index (%)	60.32 ± 27.33	28.3 (14.4, 46.25)	11.1 (3.6, 41.7)	<0.001	<0.001	0.75	0.786
ITC Area (mm ²)	12.91 ± 9.76	1.97 (0.77, 6.01)	0.69 (0.05, 4.32)	<0.001	<0.001	0.749	0.768
CCT (um)	548.04 ± 34.19	541.3 ± 26.61	544.0 (506.0, 572.0)	0.882	0.059	0.526	0.281
ACD (mm)	1.49 ± 0.43	2.17 ± 0.4	2.23 ± 0.57	<0.001	<0.001	0.858	0.853
ACW (mm)	11.47 ± 0.36	11.59 ± 0.33	11.57 ± 0.44	0.504	0.067	0.582	0.497
Pupil Diameter (mm)	4.86 ± 1.56	4.56 ± 0.93	4.46 ± 1.34	0.564	0.427	0.531	0.492
AL (mm)	22.8 ± 0.91	22.78 ± 0.89	23.3 (22.26, 24.4)	0.367	0.696	0.448	0.486
Crystalline lens							
R[Front] (mm)	7.92 ± 0.74	8.58 ± 0.74	9.21 ± 1.41	0.001	0.005	0.729	0.667
Rs[Front] (mm)	7.09 ± 0.38	8.05 ± 0.68	8.54 ± 1.24	<0.001	<0.001	0.889	0.823
Rf[Front] (mm)	8.75 ± 1.35	9.12 ± 0.99	9.88 ± 1.94	0.03	0.287	0.596	0.501
R[Back] (mm)	5.37 ± 0.62	5.57 ± 0.43	6.04 ± 0.76	0.002	0.055	0.56	0.621
Rs[Back] (mm)	5.06 ± 0.64	5.27 ± 0.41	5.56 ± 0.5	0.011	0.089	0.582	0.628
Rf[Back] (mm)	5.68 ± 0.68	5.87 ± 0.66	6.26 (5.6, 6.82)	0.048	0.182	0.526	0.589
Len Thickness(mm)	5.18 (5.07, 5.44)	4.88 (4.8, 5.11)	4.8 ± 0.46	0.003	<0.001	0.75	0.728
Decentration(mm)	0.19 (0.14, 0.3)	0.08 (0.05, 0.12)	0.11 (0.07, 0.17)	0.006	0.001	0.766	0.648
Tilt(deg.)	5.7 ± 3.89	5.1 ± 1.12	5.03 ± 1.26	0.597	0.526	0.452	0.442
Lens Diameter(mm)	9.91 (9.69, 10.21)	9.95 ± 0.45	10.29 ± 0.6	0.047	0.412	0.517	0.587
LV (mm)	1.45 ± 0.35	0.86 ± 0.36	0.73 ± 0.47	<0.001	<0.001	0.873	0.874

p value* were calculated by one-way ANOVA among LS, Fellow and Blank control group, except that gender was calculated by Fisher’s exact test. and age by t-test between LS patient and Cataract Patient.

p_value (LS vs F) was calculated by paired t-test or paired Wilcoxon test depending on the normality of the variable.

BCVA: best corrected visual acuity.

IOP: intraocular pressure.

C/D: cup/disk ratio.

ITC Index: iris-trabecular contact index.

ITC Area: iris-trabecular contact area.

CCT: corneal central thickness.

ACD: anterior chamber depth.

ACW: anterior chamber width.

AL: axial length.

LV: lens vault.

Rs[Front]: the anterior radius of steep curvature of the lens.

Rf[Front]:the anterior radius of flat curvature of the lens.

R[Front]: mean value of anterior R of the lens.

Rs[Back]: the posterior radius of steep curvature of the lens.

Rf[Back]:the posterior radius of flat curvature of the lens.

R[Back]: mean value of posterior R of the lens.

2.3. Data process and statistical analysis

Continuous variables were presented as mean and standard deviation or quartiles according to the normality assessed by Shapiro Wilk’s test. Univariate analysis of clinical quantitative data was performed with parametric test (Welch’s *t*-test) or nonparametric test (Wilcoxon-Mann Whitney test). Paired test comparison was used between internal control and non-paired test for comparison with cataract group. The gender was described as percentages of female. The analysis of gender data was performed with Fisher’s exact test. $p < 0.05$ was considered statistically significant. The logistic regression model with stepwise forward and backward are used to select parameters in the present study. Variance inflation factor (VIF) were considered to identify the independent predictors for diagnosis model as previous studies [21]. The threshold value of VIF was set to >10 to avoid intolerable multi-collinearity [22]. Dependent variables are excluded from the VIF calculation by its definition. Pearson correlation was performed between the expression of clinical parameters in all groups. The receiver operating characteristic (ROC) curves in logistic regression with leave one out cross-validation were conducted for area under ROC curves (AUC) score calculation. For multivariate analysis, logistic model and Gaussian Naive Bayes (GaussianNB) model were used. AUC score was calculated with leave one out cross-validation. All analysis was done with python 3.

3. Results

3.1. Characterization of basic information and morphological parameters

To characterize the basic information and morphological parameters in patients with lens subluxation (LS) using the CASIA2 system, a total of 46 participants were enrolled including 23 LS patients and 23 cataract patients. For the LS patients, their contralateral eyes without lens subluxation were used as fellow controls (F), eyes from cataract patients were identified as blank controls (B). Representative CASIA2 images were shown in Fig. S2. The demographic and basic clinical information of the three groups was shown

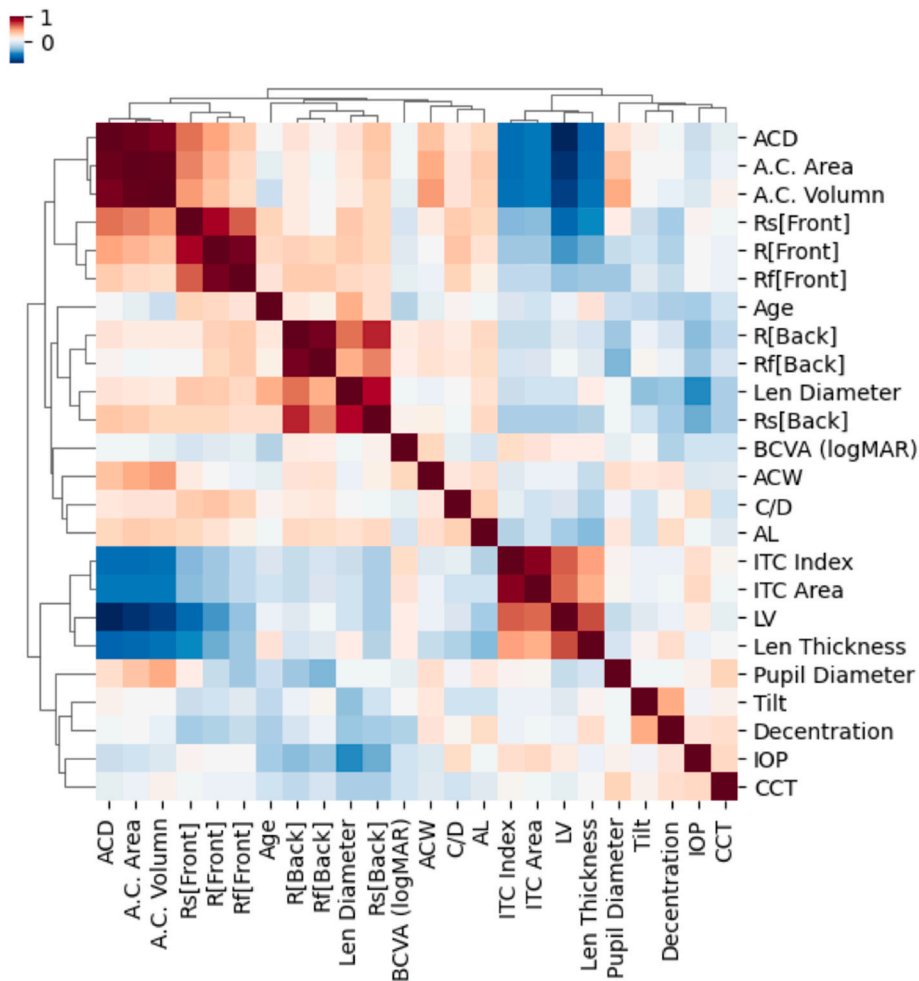


Fig. 1. Pearson correlation heatmap of the basic and morphological parameters.

in Table 1. Significant differences were found in age, BCVA, R[Front], Rs [Front], R[back], Rs[back], lens thickness, lens decentration, lens diameter, ITC index, ITC Area, ACD and LV. Pearson correlation analysis revealed that half of the parameters were clustered together into anterior chamber group, lens radius group, and lens thickness group. Moreover, the anterior chamber group parameters were found to be negatively correlated with lens thickness group parameters and slightly positively correlated with lens radius [Front] group, as shown in Fig. 1. Variance inflation factor (VIF) were calculated to identify the independent predictors for diagnosis model and shown in Fig. S3. R[Front] and Rf[Front] showed VIF score of 10.7. R[Back] and Rf[Back] showed VIF score of 10.6. So they were removed due to high VIF to avoid multi-collinearity problem. LV and ACD revealed VIF score of 6.93. All the others revealed VIF scores below 3.

3.2. Diagnostic markers comparing LS and controls

The distribution of significantly different parameters was analyzed and presented in Fig. S4. The cross-validation area under the curve (AUC) scores for the logistic regression model with leave-one-out cross-validation between LS and fellow eyes were calculated and are shown in Table 1. Corresponding ROC curves and cutoff values were displayed in Fig. S4. Among these parameters, LV, Rs [front], and ACD demonstrated the highest prediction power with AUCs of 0.87[0.77, 0.98], 0.89[0.78, 1], and 0.86[0.75, 0.96], respectively. And their statistical powers reveal over 90 % at a = 0.05. Additionally, our previous correlation analysis revealed that these parameters clustered into separate groups. The parameters including ITC Index, ITC Area, ACD, decentration, LV, len thickness, len diameter, R[Front], Rs[Front], R[Back], Rs[Back] and age were initially considered. Stepwise selection were then conducted and finally LV, Rs[front] and ACD were included in the multivariate model with high AUC of 0.92 (shown in Fig. 2A when comparing LS and F). If we include the blank control group in the analysis, the AUC score slightly decreased as shown in Fig. 2B.

3.3. Tilt presents as a sensitive diagnostic marker in GaussianNB model

In order to further enhance the prediction power, we analyzed axis-related data including lens decentration, lens tilt, Rs, and Rf axis in the present study. These parameters have not been widely studied in the past. As shown in Table 2, the statistical analysis of axis parameters showed no difference except tilt axis and Rf[back] axis. However, when the axis data were studied in a 2-dimensional (2D) map (where the OS eye was mirrored), a significant difference emerged, as shown in Fig. 3A–F. Tilt and tilt axis in the LS eye and fellow eye were clearly separated in 2D space but not in 1D, indicating that univariate analysis of axis-type data might lose information (Fig. S5). Moreover, linear/logistic regressions may not be the best method for analyzing 2D data. Therefore, we compared several methods and selected the Gaussian Naive Bayes model (GaussianNB) as the optimal one in the present study. The ROC curves of tilt/axis and 2D decision boundary map were shown in Fig. 4A and B. The prediction power of tilt/axis was much higher in the GaussianNB model (AUCs = 0.90) than in the logistic model (AUCs = 0.74). Decision boundary map showed clear cluster distribution between LS and fellow controls. A clear ellipse well captured the natural gaussian distribution of lens tilt and separate LS and Fellow eyes in two regions via GaussianNB model.

3.4. Combination of tilt and LV greatly improve the prediction power

Based on the above findings, a combination of LV, ACD, Rs[front] and axis related markers was shown to greatly improve the

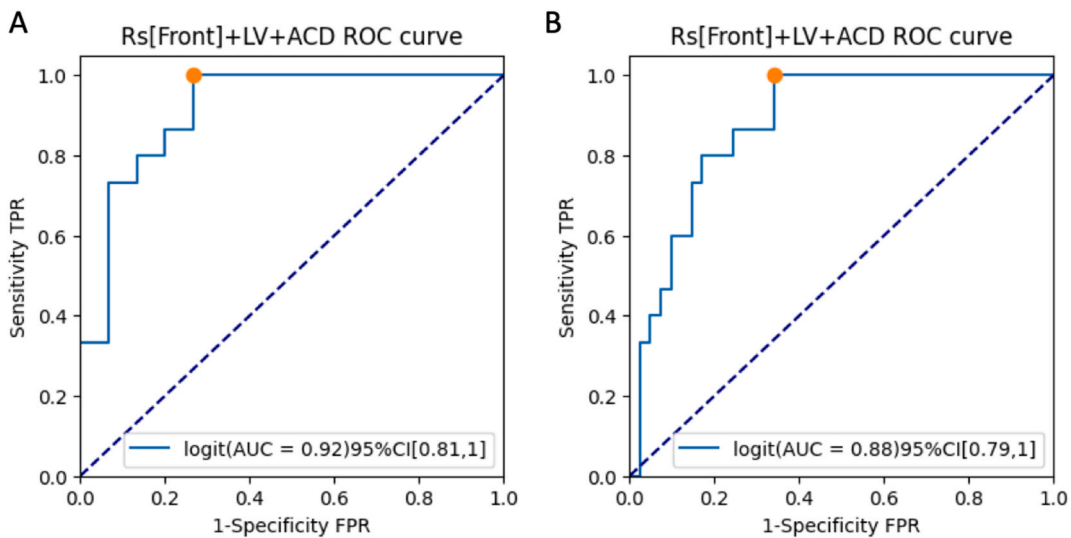


Fig. 2. Combination of Rs [Front], LV and ACD improves the prediction power. ROC curve showing the comparison between LS and Fellow eyes (A) and the comparison between LS and Fellow eyes + Blank eyes (B).

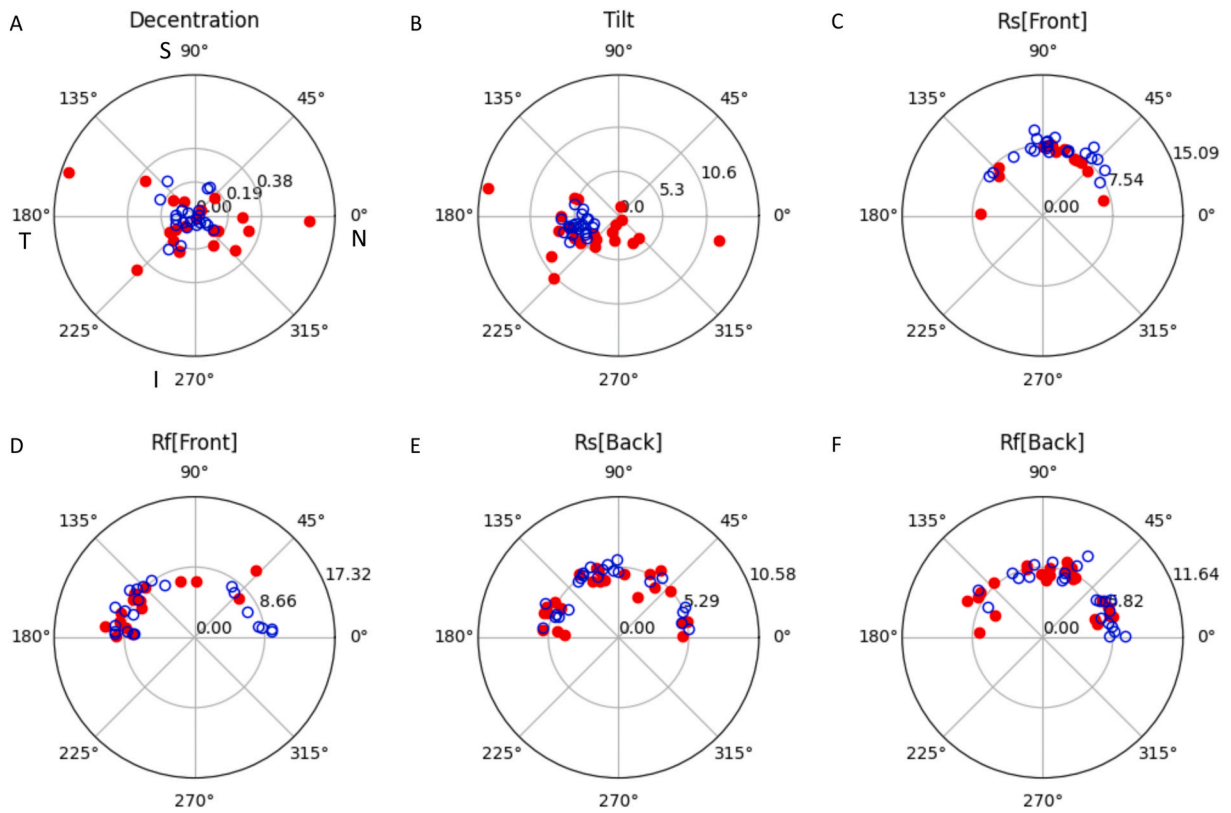


Fig. 3. Illustration of the 2D distribution of axis-related parameters between LS and Fellow eyes. In the polar coordinates, Radius represents variables (e.g. Tilt). Degree represents the axis of the variables (e.g. Tilt axis). Red dots represent LS eyes and blue circles represent Fellow eyes. (For interpretation of the references to color in this figure legend, the reader is referred to the Web version of this article.)

Table 2

The axis-related information of the included eyes.

	LS	Fellow(F)	Blank(B)	p_value*	p_value (LS vs F)	AUC (LS vs F)	AUC (LS vs F + B)
Decentration(mm)	0.19 (0.14, 0.3)	0.08 (0.05, 0.12)	0.11 (0.07, 0.17)	0.006	0.001	0.766	0.648
Decentration Axis (Deg.)	233.0 ± 96.15	197.38 ± 88.8	170.45 ± 91.22	0.101	0.147	0.567	0.607
Tilt(Deg.)	5.7 ± 3.89	5.1 ± 1.12	5.03 ± 1.26	0.597	0.526	0.452	0.442
Tilt Axis(Deg.)	223.05 ± 61.42	192.9 ± 12.08	192.55 ± 19.03	0.016	0.036	0.705	0.691
Rs[Front] (mm)	7.09 ± 0.38	8.05 ± 0.68	8.54 ± 1.24	<0.001	<0.001	0.889	0.823
Rs Axis[Front] (Deg.)	81.8 ± 40.98	78.2 ± 28.48	82.42 ± 39.29	0.941	0.75	0.307	0.049
Rf[Front] (mm)	8.75 ± 1.35	9.12 ± 0.99	9.88 ± 1.94	0.03	0.287	0.596	0.501
Rf Axis[Front] (Deg.)	148.0 (119.5, 170.0)	144.0 (90.5, 165.0)	105.0 (26.5, 143.0)	0.062	0.847	0.462	0.567
Rs[Back] (mm)	5.06 ± 0.64	5.27 ± 0.41	5.56 ± 0.5	0.011	0.089	0.582	0.628
Rs Axis[Back] (Deg.)	103.0 ± 55.9	101.39 ± 50.46	129.5 (61.5, 163.0)	0.705	0.902	0.243	0.225
Rf[Back] (mm)	5.68 ± 0.68	5.87 ± 0.66	6.26 (5.6, 6.82)	0.048	0.182	0.526	0.589
Rf Axis[Back] (Deg.)	83.43 ± 49.87	58.35 ± 45.84	101.6 ± 43.19	0.012	0.136	0.578	0.269

p value* were calculated by one-way ANOVA among LS, Fellow and Blank control group.

p_value (LS vs F) was calculated by paired t-test or paired Wilcoxon test depending on the normality of the variable.

prediction power. To further investigate the best marker sets, we tried the combinations and found a three-parameter model (LV, tilt, and tilt axis) analyzed via GaussianNB model (3p GaussianNB model) achieved the highest AUC score of 0.95 (Fig. 5A and Fig. S7). Additionally, when we extended the data to include blank controls for a general circumstance, the prediction power increased to an AUC score of 0.97 (Fig. 5B and Fig. S7), indicating them as a good combination.

Moreover, asymmetric anterior chamber depth was widely reported to suggest lens subluxation in clinics [2]. To address this issue, we add ACD_std and LV_std via CASIA2 system which is the difference of ACD and LV values among 360-degree angles (Fig. S6). The

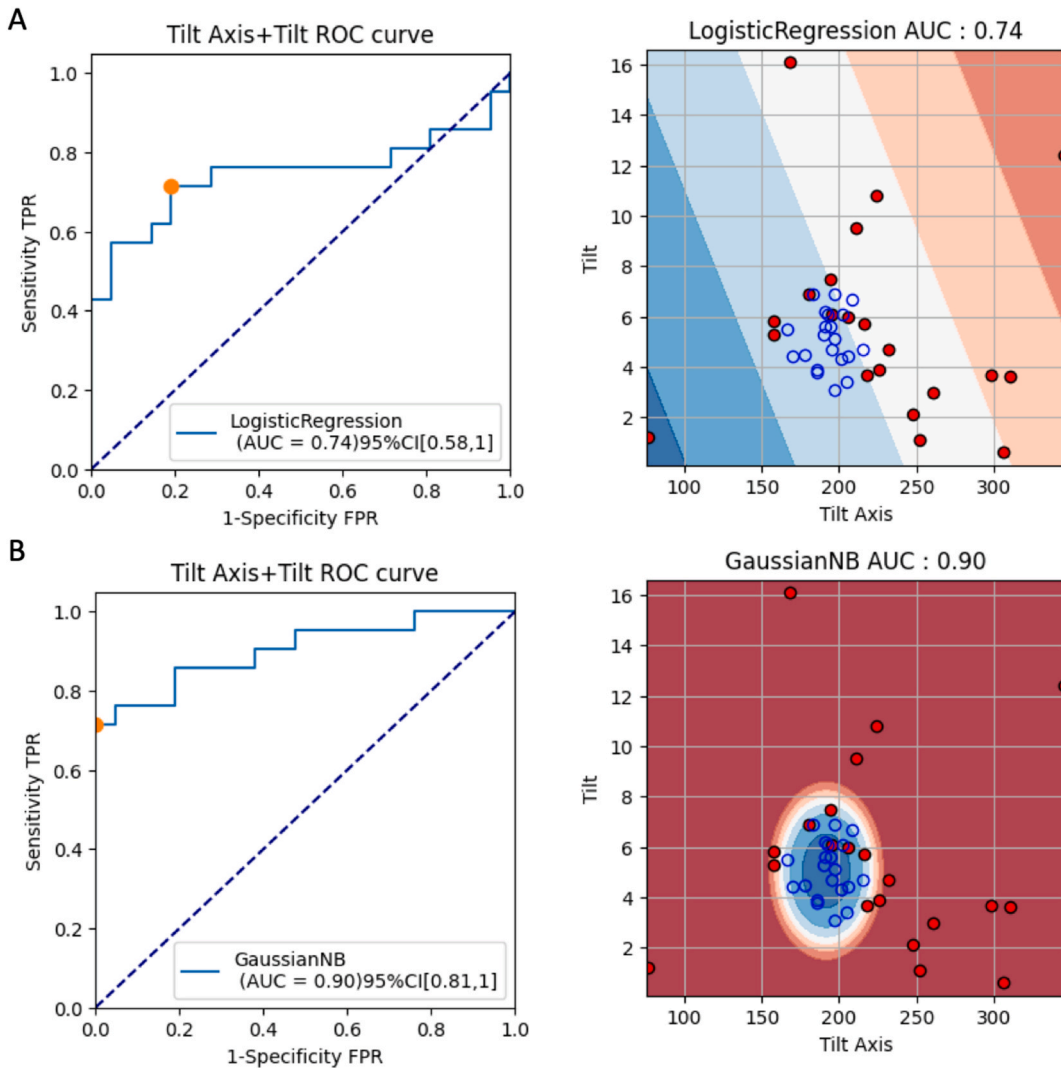


Fig. 4. The ROC curve and decision boundary map of tilt and tilt axis in logistic regression model and GaussianNB model between LS and Fellow eyes. The topology view showed clear cluster distribution between LS and fellow controls. Red dots represent LS eye and blue circles represent Fellow eye. Red-blue color represents the probability of the LS and control group respectively. (For interpretation of the references to color in this figure legend, the reader is referred to the Web version of this article.)

results showed that the mean and std of ACD and LV improved the prediction power in the GaussianNB model (AUCs = 0.91, AUC = 0.91, respectively) compared to the logistic regression model (AUCs = 0.86, AUC = 0.87, respectively). Notably, when we combined LV_mean, LV_std, tilt, and tilt axis in a four-parameter GaussianNB model (4p Gaussian model), there was a prominent improvement in prediction power (AUCs = 0.98[0.94, 1]) comparing LS eyes and Fellow eyes (Fig. 5A). To further evaluate the generalization of the model, we extended the dataset to include blank controls, and the prediction power remained excellent with an AUC score of 0.98 [0.95, 1] (Fig. 5B). However, when we used ACD_mean, ACD_std, tilt and tilt axis, the prediction power was 0.89 when extended to blank controls (Fig. S7), indicating LV and tilt as the most stable and generalized combination.

4. Discussion

Similar to other previous ASOCTs, CASIA2 has revealed diverse applications in the management of the ocular diseases. It can be used to predict anterior chamber angle for phakic intraocular lens implantation with deeper, wider and faster scanning of anterior segment combined with sophisticated mathematical modeling, which could greatly reduce the risks associated with the narrowing of the anterior chamber angle postoperatively [21]. It could also be applied to assess the anterior chamber inflammation with higher resolution images [23,24]. Besides, it has been reported to predict IOL tilt and decentration in modern cataract surgery [25]. While this merit has not been widely used in clinical management. This study comprehensively and quantitatively analyzed the anterior segment and lens morphological parameters around 360-degree angles of patients with AAC secondary to LS using the CASIA2 OCT, identified

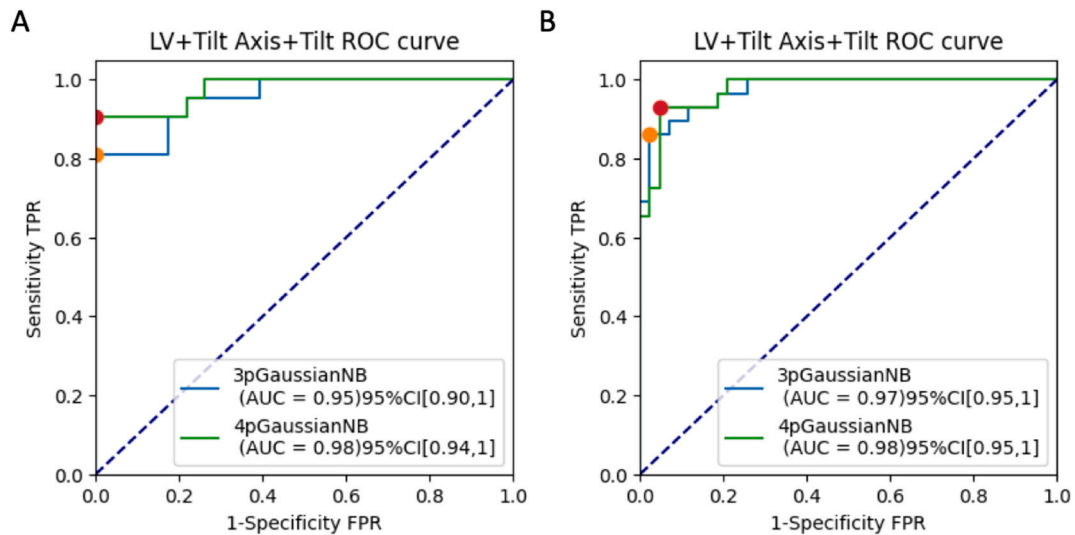


Fig. 5. Combination of tilt and LV in GaussianNB model improves the prediction power. ROC curve showing the comparison between LS and Fellow Ctrl (A) and the comparison between LS and Fellow Ctrl + Blank Ctrl (B). 3pGaussianNB model includes tilt, tilt axis and LV_mean. 4pGaussianNB model includes tilt, tilt axis, LV_mean and LV_std.

significant different parameters and highlighted the role of LV and tilt in the diagnosis of these patients. The results demonstrated the combination of LV_mean, LV_std, tilt and tilt axis in GaussianNB model as excellent diagnostic markers for LS (AUCs = 0.98). This combination of markers and the mathematic model provides novel diagnostic indications for LS.

Asymmetrical ACD were widely studied and recognized in the diagnosis of LS. Previous studies [2] reported shallower ACD and larger ACD differences between contralateral eyes in patients with AAC associated with lens subluxation. The reported AUCs for ACD and ACD difference was 0.763 and 0.966 respectively without cross-validation. We also found in our study that LV, ACD, Rs [Front] were significantly different between LS and fellow eyes. However, the prediction power of ACD, Rs [Front] decreased when considering cataract blank controls. This might be explained that the age of patients in blank group was older than that in LS patients. ACD decreased with the development of cataract, thus the prediction power of ACD for LS in older patients with cataract would decrease. Meanwhile, as we recruited LS patients with asymmetrical distance between ciliary body and crystalline lens in different quadrants under UBM, the key characterization of these LS eyes is actually shallower ACD or increased tilt of crystalline lens in the weak area of zonules, the central ACD may not be absolutely shallow, indicating LV and tilt are more stable in this situation.

Consensus has been reached that abnormal lens position due to zonulopathy is one of the pathogenesis of primary angle closure glaucoma (PACG) [26,27]. Approximately 18 % acute angle closure [5] or PACG [8] are reported to have spontaneous lens dislocation, and about 6 % acute angle-closure glaucoma secondary to lens subluxation were reported to be misdiagnosed as acute PACG [8,9]. What's more, the incidence of uneven zonular laxity in PACG patients undergoing cataract surgery can reach to more than 20 %, even as high as 58 %, which is difficult to evaluate accurately in preoperatively. Although it is difficult to identify whether zonulopathy is a causative or a secondary change in AAC, unveiling the mechanism of zonulopathy underlying angle closure glaucoma and identifying sensitive imaging indicators are of significant clinical implications. Efforts have been made on UBM images to investigate zonular damage [5,6,11,28]. Iris lens angle and non-forward convexity of iris were reported as sensitive and characteristic indexes for screening lens subluxation and zonular rupture [5]. The present study highlighted the role of LV and lens tilt as sensitive and stable indicators for patients with AAC secondary to LS via ASOCT, and we believe it might have something to do with the mechanism of AAC in these eyes.

Lens subluxations were known to be induced by partial dysplasia, rupture or laxity of zonules etc. However, our current understanding is that the position of the crystalline lens is not only restricted by lens zonules, but also restricted by vitreous anterior limiting membrane through Weigert's zonules and vitreous zonules. Meanwhile, it dynamically changes during the accommodation of ciliary body, and moves forward or backward with the alteration of vitreous pressure, which could be more dramatic when zonulopathy exists. Thus, we hypothesize that the position of the crystalline lens is determined by the ciliary body-zonules-crystalline lens-vitreous anterior limiting membrane-anterior vitreous complex (CZLMV). When the structure or function of the CZLMV complex is integrated, the position of the lens is dynamically balanced. The dysregulation of any part of the complex would lead to the imbalance of the surrounding forces, resulting in abnormal position or morphology. Once LS occurs, the balance around the crystalline lens was disrupted, which could trigger misdirection of the aqueous humor [29]. In this process, the connection between the lens posterior capsule, Weigert's zonules, vitreous zonules and vitreous anterior membrane are also affected, resulting in the accumulation of aqueous humor in the Berger area behind the crystalline lens and even in the vitreous, which could further cause a high pressure behind the complex and then push the complex forward. If lens zonules are partially ruptured or defected, the increased pressure behind the complex would unavoidably lead to the forward movement of the anterior vitreous, cause vitreous block at the circumferential space, even forming vitreous hernia at the weak part, and then result in the increased tilt of the crystalline lens, increased LV_mean and LV_std,

asymmetrical ACD and peripheral anterior chamber depth in the LS direction. When this happened, the misdirection of the aqueous humor could enter into a vicious circle, and the remaining intact lens zonules might be stretched during this process and get looser or ruptured as it did in PACG with secondary zonulopathy [30]. This would further push the complex forward and progress to acute angle closure or even malignant glaucoma [31]. Moreover, our data showed that LV is positively correlated with the ITC index and ITC area, reflecting the association of LV with the onset of ACG. These parameters indirectly reflect the status of the zonules and indeed provide us new insights into understanding the pathogenesis of angle closure secondary to LS.

Furthermore, early and accurate detection of the dimension of LS by LV and tilt could indicate clinical treatment and help achieve better clinical outcomes. If patients are diagnosed with LS or abnormal zonular ligaments, capsular retractors and capsule tension ring (CTR) implantation are often considered to stabilize the capsular bag, especially for patients with zonular rupture range $<180^\circ$ [32, 33]. For those with zonular rupture >2 quadrants, phacoemulsification combined with capsular tension segment or implantable capsular hooks and IOL implantation would be recommended, IOL suspension can also be selected [30]. Meanwhile, we should be alert during cataract surgery that the remaining unruptured lens zonules under UBM and ASOCT might also be loose or fragile in patients with AAC secondary to LS. Therefore, LS eyes should be treated before AAC developed.

As novel parameters to evaluate the position of crystalline lens or intraocular lens, tilt and decentration have been widely studied in age-related cataract cases [13,14]. Our data are consistent with previous studies [13,14] that preoperative crystalline lens tend to tilt approximately 5° towards the inferotemporal direction (193°). Although the 3p or 4p GaussianNB model criteria boundary can't be viewed intuitively. The normal tilt angle is approximately in an ellipse area with the following formular $[(Tilt - M_1)/R_1]^2 + [(Tilt\ axis - M_2)/R_2]^2 \leq 1$, where $M_1 \sim 5^\circ$, $M_2 \sim 193^\circ$, $R_1 \sim 2^\circ$, $R_2 \sim 23^\circ$. Chen et al. reported that lens tilt is positively correlated with lens decentration and negatively correlated with AL [14]. However, no difference was found in AL among LS, Fellow, and Blank controls in the present study. Lens decentration is also an important factor for crystalline lens and supposed to be indicative for lens subluxation, but based on our results, the prediction power of decentration was not high in either logistic model or Gaussian model. The reason might be that decentration is closely associated with the degree of LS and the imbalanced forces around all directions. The patients enrolled in our study were patients with AAC secondary to LS and the LS diagnosed by UBM were probably the partial rupture or laxity of zonules. Therefore, the crystalline lens might still be restricted by the remaining zonules and vitreous zonules, resulting in no difference in lens decentration. While the rupture or laxity of zonules forms a weak area of zonules, which would lead to an increase of tilt and LV in the LS direction during the process of vitreous block as mentioned previously. These also imply the crucial role of vitreous on the pathogenesis of AAC secondary to lens subluxation.

Although the present study provides novel and stable diagnostic markers for eyes with AAC secondary to LS and facilitates clinical work. There are some limitations. First, the sample size of the study is small, and we lack the independent validation process, but we had strict inclusion criteria for LS eyes and controls, that is why we had significantly different results among groups and identified the most sensitive parameters in this study. Second, the acute attack of AAC and whether it had been relieved before the AS-OCT examination would add in confounding factors when evaluating the morphological parameters. Future studies that explore the differences of morphological parameters between the acute attack stage and relieved stage of AAC secondary to LS will give us more information on understanding the pathogenesis and its dynamic process for angle closure. Third, although our study defined the AAC secondary to LS by UBM diagnosis showing asymmetrical distance between ciliary body and crystalline lens in different quadrants together with shallow central and peripheral anterior chamber depth, tilting of lens, asymmetrical ACD in the same eye, and/or asymmetrical iris configuration. We can't rule out those eyes with secondary LS caused by APAC, which were also reported to have spontaneous lens dislocation. However, our results improve our understanding of the pathogenic role of zonulopathy in angle closure glaucoma.

In conclusion, the present study quantitatively analyzed anterior chamber and crystalline lens parameters, developed a stable and accurate method to diagnose lens subluxation and demonstrated the combination of LV_mean, LV_std, tilt and tilt axis in GaussianNB model as excellent diagnostic markers for AAC secondary to LS with high AUC value of 0.98. It adds to the field of imaging diagnosis of lens subluxation and benefit the clinical work by offering early detection, accurate diagnosis, prompt treatment, as well as improving our understanding of the mechanism and management of angle closure glaucoma secondary to LS.

Ethical approval

The study was approved by the Ethics Committee of Clinical Research in Beijing Tongren Hospital and all the information of the patients was kept confidential in the study.

Funding

This work was supported by National Natural Science Foundation of China (Grant No.82171050 and Grant No.82201174), Capital's Funds for Health Improvement and Research (No.2020-4-2059) and Beijing Natural Science Foundation (7232025). The authors declared no conflict of interest and no financial disclosures.

Additional information

No additional information is available for this paper.

Data availability statement

Data will be made available on request.

CRediT authorship contribution statement

Yizhen Tang: Writing – review & editing, Writing – original draft, Software, Methodology, Investigation, Funding acquisition, Conceptualization. **Yan Gao:** Software, Methodology, Investigation, Formal analysis, Data curation. **Xiaowei Yu:** Methodology, Investigation, Formal analysis, Data curation. **Hongyu Zhong:** Investigation, Data curation. **Guanchen Gong:** Investigation, Formal analysis, Data curation. **Feng Mei:** Investigation, Data curation. **Zhigang Fan:** Writing – review & editing, Supervision, Resources, Funding acquisition, Conceptualization. **Yan Shi:** Writing – review & editing, Validation, Supervision, Funding acquisition, Conceptualization.

Declaration of competing interest

The authors declare that they have no known competing financial interests or personal relationships that could have appeared to influence the work reported in this paper.

Acknowledgements

We thank Tengyang Sun and Caixia Lin of Beijing Tongren Hospital for great help in patients collecting and management, we thank Wenli Yang and Dongjun Li of Beijing Tongren Hospital for assistant in UBM and ASOCT imaging and analysis.

Appendix A. Supplementary data

Supplementary data to this article can be found online at <https://doi.org/10.1016/j.heliyon.2024.e25164>.

References

- [1] W.H. Jarrett II, Dislocation of the lens. A study of 166 hospitalized cases, *Arch Ophthalmol.* Sep 78 (3) (1967) 289–296, <https://doi.org/10.1001/archoph.1967.00980030291006>.
- [2] Q. Jing, T. Chen, Z. Chen, L. Lan, C. Zhao, Y. Jiang, Ocular manifestations of acute secondary angle closure associated with lens subluxation, *Front. Med.* 8 (2021) 738745, <https://doi.org/10.3389/fmed.2021.738745>.
- [3] L. Ning, Y. Wen, L. Lan, et al., Effect of different preoperative intraocular pressures on the prognosis of traumatic cyclodialysis cleft associated with lens subluxation, *Ophthalmol Ther.* Apr 11 (2) (2022) 689–699, <https://doi.org/10.1007/s40123-022-00468-0>.
- [4] M. Shi, L. Ma, J. Zhang, Q. Yan, Role of 25 MHz ultrasound biomicroscopy in the detection of subluxated lenses, *J Ophthalmol* 2018 (2018) 3760280, <https://doi.org/10.1155/2018/3760280>.
- [5] F. Wang, D. Wang, L. Wang, Characteristic manifestations regarding ultrasound biomicroscopy morphological data in the diagnosis of acute angle closure secondary to lens subluxation, *BioMed Res. Int.* 2019 (2019) 7472195, <https://doi.org/10.1155/2019/7472195>.
- [6] A. Wang, D. Mou, N. Wang, H. Wang, The imaging characteristics of lens subluxation on the ultrasound biomicroscopy, *Contrast Media Mol. Imaging* 2022 (2022) 7030866, <https://doi.org/10.1155/2022/7030866>.
- [7] C.Y. Qiao, H. Zhang, Y. Zhang, et al., Comparison study for the proportion of underdiagnosed zonulopathy in angle closure glaucoma, *Zhonghua Yan Ke Za Zhi.* Nov 11 58 (11) (2022) 872–881, <https://doi.org/10.3760/cma.j.cn112142-20211226-00608>.
- [8] Y. Zhang, Y. Zong, Y. Jiang, C. Jiang, Y. Lu, X. Zhu, Clinical features and efficacy of lens surgery in patients with lens subluxation misdiagnosed as primary angle-closure glaucoma, *Curr Eye Res.* Apr 44 (4) (2019) 393–398, <https://doi.org/10.1080/02713683.2018.1548130>.
- [9] L. Luo, M. Li, Y. Zhong, B. Cheng, X. Liu, Evaluation of secondary glaucoma associated with subluxated lens misdiagnosed as acute primary angle-closure glaucoma, *J. Glaucoma* 22 (4) (2013) 307–310, <https://doi.org/10.1097/JG.0b013e318241b85b>.
- [10] Z. Yu, F. Wang, F. Dong, N. Li, D. Wang, L. Wang, Comparison of ocular morphological parameters related to lens position by anterior segment optical coherence tomography and ultrasound biomicroscopy, *Int. J. Clin. Pract.* 2022 (2022) 7599631, <https://doi.org/10.1155/2022/7599631>.
- [11] J.A. McWhae, A.C. Crichton, M. Rinke, Ultrasound biomicroscopy for the assessment of zonules after ocular trauma, *Ophthalmology.* Jul 110 (7) (2003) 1340–1343, [https://doi.org/10.1016/S0161-6420\(03\)00464-0](https://doi.org/10.1016/S0161-6420(03)00464-0).
- [12] G. Calzetti, C. Bellucci, S.A. Tedesco, M. Rossi, S. Gandolfi, P. Mora, Tilt and decentration of posterior and anterior iris-claw intraocular lenses: a pilot study using anterior segment optical coherence tomography, *BMC Ophthalmol.* 22 (1) (May 23 2022) 233, <https://doi.org/10.1186/s12886-022-02430-x>.
- [13] X. Gu, X. Chen, G. Yang, et al., Determinants of intraocular lens tilt and decentration after cataract surgery, *Ann Transl Med.* Aug 8 (15) (2020) 921, <https://doi.org/10.21037/atm-20-1008>.
- [14] X. Chen, X. Gu, W. Wang, et al., Distributions of crystalline lens tilt and decentration and associated factors in age-related cataract, *J. Cataract Refract. Surg.* 47 (10) (Oct 01 2021) 1296–1301, <https://doi.org/10.1097/j.jcrs.0000000000000631>.
- [15] X. Wang, X. Chen, Y. Tang, J. Wang, Y. Chen, X. Sun, Morphologic features of crystalline lens in patients with primary angle closure disease observed by CASIA 2 optical coherence tomography, *Invest. Ophthalmol. Vis. Sci.* 61 (5) (May 11 2020) 40, <https://doi.org/10.1167/iovs.61.5.40>.
- [16] X. Chen, X. Wang, Y. Tang, X. Sun, Y. Chen, Optical coherence tomography analysis of anterior segment parameters before and after laser peripheral iridotomy in primary angle-closure suspects by using CASIA2, *BMC Ophthalmol.* 22 (1) (2022) 144, <https://doi.org/10.1186/s12886-022-02366-2>. Mar 28.
- [17] S.W. Ho, M. Baskaran, C. Zheng, et al., Swept source optical coherence tomography measurement of the iris-trabecular contact (ITC) index: a new parameter for angle closure, *Graefes Arch. Clin. Exp. Ophthalmol.* 251 (4) (Apr 2013) 1205–1211, <https://doi.org/10.1007/s00417-012-2158-6>.
- [18] T.A. Tun, M. Baskaran, S.A. Perera, H.M. Htoon, T. Aung, R. Husain, Swept-source optical coherence tomography assessment of iris-trabecular contact after phacoemulsification with or without goniosynechialysis in eyes with primary angle closure glaucoma, *Br. J. Ophthalmol.* 99 (7) (Jul 2015) 927–931, <https://doi.org/10.1136/bjophthalmol-2014-306223>.
- [19] H. Selvan, D. Angmo, A.S. Tomar, S. Yadav, A. Sharma, T. Dada, Changes in intraocular pressure and angle status after phacoemulsification in primary angle closure hypertension, *J. Glaucoma,* Feb 28 (2) (2019) 105–110, <https://doi.org/10.1097/JG.0000000000001137>.

- [20] S. Kimura, Y. Morizane, Y. Shiode, et al., Assessment of tilt and decentration of crystalline lens and intraocular lens relative to the corneal topographic axis using anterior segment optical coherence tomography, *PLoS One* 12 (9) (2017) e0184066, <https://doi.org/10.1371/journal.pone.0184066>.
- [21] H. Choi, T. Kim, S.J. Kim, et al., Predicting postoperative anterior chamber angle for phakic intraocular lens implantation using preoperative anterior segment metrics, *Transl Vis Sci Technol* 12 (1) (Jan 3 2023) 10, <https://doi.org/10.1167/tvst.12.1.10>.
- [22] D. Witten, G. James, *An Introduction to Statistical Learning with Applications in R*, springer publication, 2013.
- [23] K. Etherton, J.S. Rahi, H. Petrushkin, et al., Quantitative and qualitative assessment of anterior segment optical coherence tomography capture of disease state in childhood anterior uveitis, *Br J Ophthalmol.* Jul 107 (7) (2023) 966–972, <https://doi.org/10.1136/bjophthalmol-2021-320448>.
- [24] M. Lu, X. Wang, L. Lei, et al., Quantitative analysis of anterior chamber inflammation using the novel CASIA2 optical coherence tomography, *Am J Ophthalmol.* Aug 216 (2020) 59–68, <https://doi.org/10.1016/j.ajo.2020.03.032>.
- [25] A. Langenbacher, N. Szentmáry, A. Cayless, J. Wendelstein, P. Hoffmann, Prediction of IOL decentration, tilt and axial position using anterior segment OCT data, *Graefes Arch. Clin. Exp. Ophthalmol.* (Sep 1 2023), <https://doi.org/10.1007/s00417-023-06208-9>.
- [26] Glaucoma Group BoO, Chinese Medical Association Expert consensus on the diagnosis and treatment of primary angle-closure glaucoma in China (2019) [J], *Zhonghua Yan Ke Za Zhi* 55 (5) (2019) 325, 328.
- [27] L. Tang, N.L. Wang, N. Fan, X.Y. Liu, Angle-closure glaucoma and lens suspensory ligament: re-evaluation, *Ophthalmol CHN* 31 (3) (2022) 169–174, <https://doi.org/10.13281/j.cnki.issn.1004-4469.2022.03.002>.
- [28] S. Yaguchi, Y. Yagi-Yaguchi, T. Kozawa, H. Bissen-Miyajima, Objective classification of zonular weakness based on lens movement at the start of capsulorhexis, *PLoS One* 12 (4) (2017) e0176169, <https://doi.org/10.1371/journal.pone.0176169>.
- [29] M.A. Croft, T.M. Nork, J.P. McDonald, A. Katz, E. Lütjen-Drecoll, P.L. Kaufman, Accommodative movements of the vitreous membrane, choroid, and sclera in young and presbyopic human and nonhuman primate eyes, *Invest Ophthalmol Vis Sci.* Jul 26 54 (7) (2013) 5049–5058, <https://doi.org/10.1167/iovs.12-10847>.
- [30] H. Zhang, Y. Zhang, S. Zhang, C.Y. Qiao, Lens zonulopathy and primary angle closure glaucoma: what we know and what we don't know, *Eye Sci.* 38 (2) (2023) 140–147, [10.12419/j.issn.1000-4432.2023.02.10](https://doi.org/10.12419/j.issn.1000-4432.2023.02.10).
- [31] P.A. Chandler, W.M. Grant, Mydriatic-cycloplegic treatment in malignant glaucoma, *Arch Ophthalmol.* Sep 68 (1962) 353–359, <https://doi.org/10.1001/archophth.1962.00960030357010>.
- [32] N. Fan, N.L. Wang, X.Y. Liu, Angle-closure like glaucoma secondary to lens suspensory ligament laxity, *Ophthalmology in China* 27 (2018) 4–8, <https://doi.org/10.13281/j.cnki.issn.1004-4469.2018.01.002>.
- [33] C.H. Weber, R.J. Cionni, All about capsular tension rings, *Curr Opin Ophthalmol.* Jan 26 (1) (2015) 10–15, <https://doi.org/10.1097/icu.0000000000000118>.